PHYSICAL REVIEW E **94**, 060401(R) (2016)

Fronts under arrest: Nonlocal boundary dynamics in biology

Scott G. McCalla and James H. von Brecht
Department of Mathematical Sciences, MSU, Bozeman, Montana 59717, USA
and Department of Mathematics and Statistics, CSULB, Long Beach, California 90840, USA
(Received 27 May 2016; revised manuscript received 11 October 2016; published 29 December 2016)

We introduce a minimal geometric partial differential equation framework to understand pattern formation from interacting, counterpropagating fronts. Our approach concentrates on the interfaces between different states in a system, and relies on both nonlocal interactions and mean-curvature flow to track their evolution. As an illustration, we use this approach to describe a phenomenon in bacterial colony formation wherein sibling colonies can arrest each other's growth. This arrested motion leads to static separations between healthy, growing colonies. As our minimal model faithfully recovers the geometry of these competing colonies, it captures and elucidates the key leading-order mechanisms responsible for such patterned growth.

DOI: 10.1103/PhysRevE.94.060401

Nonlocality has recently crystallized into an essential component of the mathematical study of biological pattern formation. A variety of natural mechanisms lead to nonlocal effects: An animal's ability to see and hear its surroundings leads to convolutional averages in swarming, aggregation, and alignment models of collective behavior [1–7]; the propensity of a species to broadly forage according to superdiffusive processes, such as Lévy flights, motivates the use of fractional Laplacians in partial differential equation (PDE) models of albatrosses, sharks, and criminals [8–11]; the physical coupling between neurons also leads to nonlocal operators in continuum models for nerve signal propagation and hallucinations [12–15]. Even local PDEs used for understanding phase transitions and optics, such as the Allen-Cahn equation and singularly perturbed reaction-diffusion systems, exhibit an effective nonlocal coupling at the interface between different domain boundaries [16–18].

Despite the recent deluge of mathematical models that exploit nonlocality, there still remains a broad class of interesting biological phenomena where nonlocal models could provide significant insight. These broadly fall into the category of complex systems characterized by the presence of several sharp, *mutually interacting* codimension one interfaces or fronts; see Fig. 1. These systems represent biological analogs of well-studied physical systems, such as the motion of incompressible vortex patches and vortex sheets [19,20]. Just as the presence of sharp, discontinuous jumps between regions of different vorticity naturally leads to a nonlocal evolution equation for the motion of the front, such as the Birkhoff-Rott equation in the case of a vortex sheet, the mutual interactions between fronts in biological systems lead to an analogous class of nonlocal evolution laws. Despite the successful history of nonlocal contour dynamics in fluid dynamics and material science, this approach appears underused as a tool for understanding pattern formation in biological systems.

We exploit the analogy between biological fronts and domain boundaries in material science to understand a specific pattern forming mechanism wherein the interactions between a collection of counterpropagating, or driven, codimension one fronts lead to a cessation of forward motion. We refer to these as arrested fronts. We study the motion of these interfaces under the influence of nonlinear, nonlocal interactions that account for the repulsive forces induced by the other members in the collection. This nonlocality proves crucial for describing the arrested front phenomenon. In contrast to the more standard methodology, based on coupled systems of reaction-diffusion equations with multiple scales, our approach provides a flexible, minimalistic way to study arrested fronts. From both an analytical and computational perspective, this framework offers reduced model complexity while still capturing the essential pattern forming mechanisms.

The motivation for this approach arises out of a well-established body of literature that reduces the evolution of multicomponent reaction-diffusion systems to that of codimension one interfaces via contour dynamics [21–24]. These reduced equations typically describe geometric motion of the interfaces, and can also include nonlocal self-interactions in certain cases. We view this class of reduced equations as primary models that, even if they are not necessarily tied to an underlying reaction-diffusion system, are interesting and useful in their own right. This viewpoint provides the impetus to broaden their functional form and domain of application. Crucially, this insight allows us to naturally arrive at a cohesive description of a *mutually interacting* collection of codimension one interfaces. We provide an example application of this approach that models the two-dimensional bacterial growth of competing sibling bacteria colonies, but we emphasize that the framework easily extends to higher dimensional settings and to far more general situations. We therefore conclude with a summary of physical problems to which this methodology applies.

A framework for arrested fronts. Our general class of models describes the dynamics of a collection $\mathcal{C} = \{\gamma^1, \ldots, \gamma^N\}$ of N mutually interacting planar curves

$$\gamma^i(x,t) = \begin{bmatrix} \gamma_1^i(x,t) \\ \gamma_2^i(x,t) \end{bmatrix}, \quad \gamma^i(x,t) : D \times \mathbb{R}^+ \mapsto \mathbb{R}^2,$$

where D denotes some fixed Lagrangian coordinate domain. We assume that the nonlocal force $\mathbf{v}_{\mathrm{NL}}^i(x,t)$ on $\gamma^i(x,t)$ always acts in some *a priori* known direction $\mathfrak{d}^i(x,t)$ to leading order. Its magnitude varies under the influence of self-repulsion and repulsive-attractive effects induced by the remaining curves $\gamma^j \in \mathcal{C}$ in the collection. These assumptions lead to a nonlocal velocity field $\mathbf{v}_{\mathrm{NL}}^i(x,t) := v_{\mathrm{NL}}^i(x,t)\mathfrak{d}^i(x,t)$ with

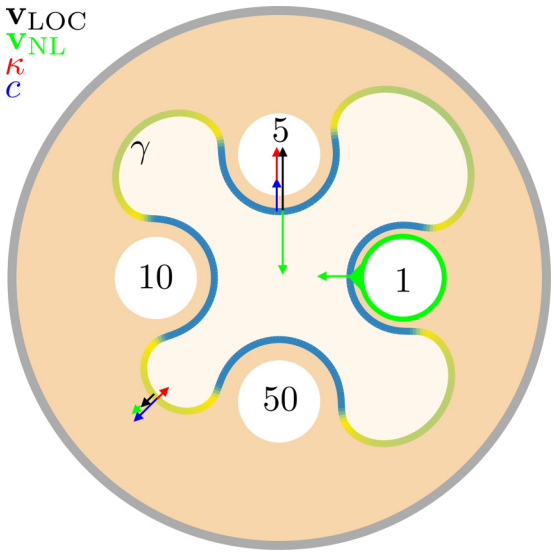

FIG. 1. Graphical depiction of (1) for a single bacterial colony. The boundary γ of the colony evolves according to pure normal motion. Pointwise curvature κ_γ and a constant normal velocity c give the total local component $\mathbf{v}_{\mathrm{LOC}}$ of the normal velocity. The repulsive nonlocal term $\mathbf{v}_{\mathrm{NL}}$ arises from integrating an interaction kernel around the boundary of each white circle. The number on each circle indicates the strength of the kernel; the green (light gray) overlay on circle 1 emphasizes the boundary of integration for the nonlocal term. The color along γ depicts the total velocity at each point; points with zero velocity (in blue or dark gray) form the arrested portions of the colony. The separation between the colony edge and the circular boundaries increases with the strength (1–50) of the nonlocal interaction.

magnitude $v^i_{\mathrm{NL}}(x,t) :=$

$$\oint_D f_i\left(\frac{1}{2}|\gamma^i(x,t)-\gamma^i(z,t)|^2\right)|\partial_x\gamma^i(z,t)|dz + \sum_{j\neq i}\oint_D g_{ij}\left(\frac{1}{2}|\gamma^i(x,t)-\gamma^j(z,t)|^2\right)|\partial_x\gamma^j(z,t)|dz.$$

The kernels $f_i(s)$ describe the self-interaction of γ^i, while $g_{ij}(s)$ describes the influence of γ^j on γ^i due to nonlocality. In addition to this nonlocal forcing, we assume each of these interfaces undergoes an additional geometric motion driven by a combination of curvature $\kappa_{\gamma^i}(x,t)$ and constant normal growth. These considerations lead to the following general class

$$\partial_t\gamma^i(x,t) = [\epsilon^i\kappa_{\gamma^i}(x,t)+c^i]\mathfrak{n}_{\gamma^i}(x,t)+\mathbf{v}^i_{\mathrm{NL}}(x,t) \qquad (1)$$

of front evolutions, provided we let $\mathfrak{n}_{\gamma^i}(x,t)$ denote the outward unit normal vector to each curve. See Fig. 1 for a graphical depiction of this type of evolution.

The model parameters include the functional forms of the nonlocal kernels $f_i(s), g_{ij}(s)$, the relative strength ϵ^i of the curvature, and the constant speed c^i of normal growth. For simplicity we assume identical nonlocal interactions with Gaussian decay

$$f_i(s) = g_{ij}(s) = g_{C,\sigma}(s) := (C/\sqrt{2\pi}\sigma)e^{-s/\sigma^2} \qquad (2)$$

described by the strength C and the length scale σ parameters. By assuming identical curvature $\epsilon^i \equiv \epsilon$ and normal growth $c^i \equiv c$ parameters, we may set $\epsilon = c = 1$ via nondimensionalization. This yields a set of equations (1) governed by a single relative strength $\tilde{C} = C/c$ parameter and a single relative length scale $\tilde{\sigma} = \sigma c/\epsilon$ parameter. We omit the tildes in the remainder of this Rapid Communication.

Competing bacteria colonies. We illustrate this modeling methodology with a case study involving a well-known phenomenon in bacterial colony formation. Bacteria often secrete antibacterial compounds to inhibit the growth of competing colonies. These compounds may inhibit the growth of sibling colonies, and self-inhibition of a single colony may also occur for certain geometries. The strain *Paenibacillus dendritiformis* serves as a model bacteria for experimentally studying and mathematically modeling sibling and self-inhibition [25,26].

Previous modeling of this phenomenon exploits the classical reaction-diffusion methodology [26]. The model exhibits multiple time scales and separately tracks variables including bacterial concentration, nutrients, prespores, subtilisin (which promotes colony growth), the sibling-sibling inhibitory compound itself (i.e., sibling lethal factor or Slf), and the colony edge (see Ref. [26], Supplemental Material). All together, this leads to a system of six components in $2+1$ space-time variables with stiff dynamics due to the presence of multiple time scales. The slow variables Slf and subtilisin appear to mediate a sharp transition in the fast variable for motile bacterial concentration (see Fig. 4 in Ref. [26]). While the model faithfully reproduces the behavior of growing colonies, in terms of both sibling-sibling and self-inhibition, it proves challenging from an analytical perspective even for simple geometries.

In contrast, our general model (1) proves capable of reproducing the essential features of colony growth and is amenable to exact or asymptotic analysis. To illustrate this, we model the evolution of each bacterial colony as a front that evolves due to both local geometric effects and a nonlocal interaction with every colony. We use (1) with identical Gaussian kernels (2) to model both sibling-sibling repulsion and self-inhibition. The nonlocal forcing acts in the direction opposite to the normal $\mathfrak{d}_i(x,t) = -\mathfrak{n}_{\gamma^i}(x,t)$, so that each γ^i evolves according to pure normal motion. We set $D = (-\pi,\pi)$ with periodic boundary conditions to guarantee that each γ^i remains a simple, closed curve. In the case of a single colony, these choices lead to a governing equation that closely resembles a quasistatic reduction of the Fitzhugh-Nagumo equations in a singular parameter regime [22,23]. The nonlocality differs in form from (1), however.

We perform numerical experiments to verify that (1) suffices to describe the pattern forming behavior of *P. dendritiformis*. Specifically, we demonstrate that the model can adequately describe the geometry of evolving colonies in both sibling-sibling and self-inhibiting scenarios. We numerically integrate (1) using a simple implicit update for the curvature and an explicit update for all other forces. Figures 2 and 3 display experimental images for the colony formation from Refs. [25,27] overlaid with these numerical calculations. In the case of two colonies with circular inoculations we obtain

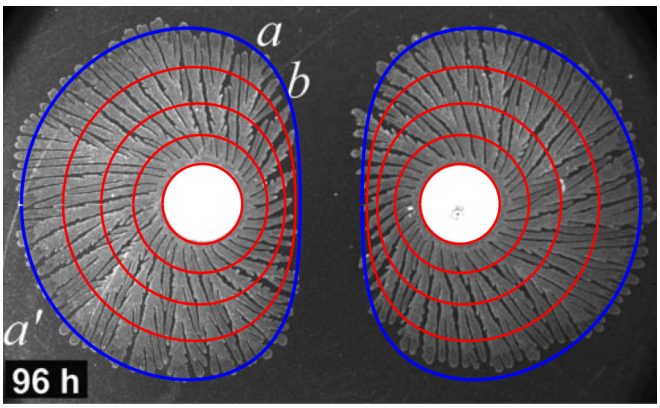

FIG. 2. Competing sibling colonies from Ref. [25], Fig. 1. Two initial inoculations, shown in white with initial radius $R_0 = 10$ and separation $s_0 = 44.2$, evolving under the dynamics of (1) and (2) with $(C,\sigma) = (0.5725, 18.45)$. The toxin produced by each colony inhibits the growth of its sibling, leading to a region of zero growth in the rectangular region between the two colonies. The red (light gray) lines and the blue (dark gray) line are successive time slices from the simulation. Curve motion arrests in the region of zero colony growth. (Figure is reproduced with permission.)

the curves in Fig. 2. These simulations show the initial onset of inhibition at a certain critical separation between the two fronts. For sufficiently large times, the interfaces between sibling colonies arrest. We perform a similar numerical experiment to qualitatively reproduce more complicated growth patterns observed in Ref. [27]. An initial inoculation of seven radial colonies is depicted in Fig. 3 to illustrate the dynamics

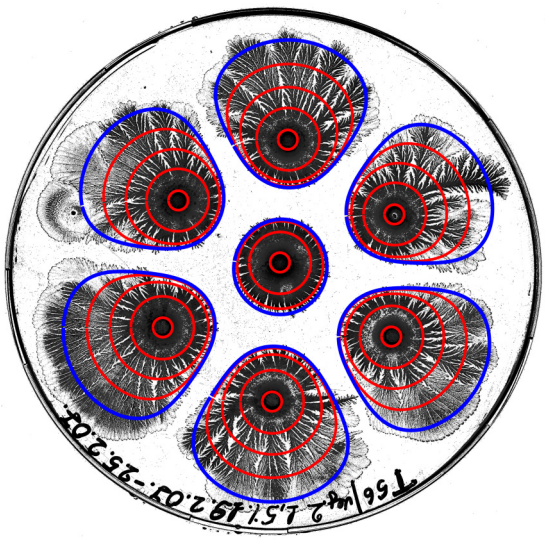

FIG. 3. Seven sibling colonies are initially inoculated in a purely radial distribution from Ref. [27]; a black and white negative of Ben-Jacob's original is shown. Six of the seven centers of each circular inoculation (small red or light gray circles) form an outer hexagonal ring surrounding the seventh circular inoculation (small red or light grey circle at center). As with Fig. 2, the red (light gray) lines and the blue (dark gray) line are time slices from a simulation of (1) using $(C,\sigma) = (0.575, 25.2)$ and a Gaussian kernel. (Figure is reproduced with permission.)

of (1) with more than two curves in the collection. In each case, (1) faithfully reproduces bacterial colony growth data at a qualitative level. In particular, the effective nonlocal repulsion and arrested nature of colony growth can clearly be seen in all of the images. These experiments demonstrate that our simplified framework (1) includes the essential features necessary to understand these arrested fronts without resorting to fully explicit modeling of numerous reaction-diffusion components.

The advantage of (1) lies in its relative simplicity. While exact solutions of (1) are unobtainable for these simulations, we may appeal to asymptotic analysis to estimate key features of these experiments. The manner in which the parameters C,σ influence the final separation s between colonies in Fig. 2 is easily estimated, for instance. After the onset of colony growth, the constant C provides a reasonable leading-order approximation of the self-interaction. We appeal to Laplace's method to estimate the nonlocal forcing from the second curve

$$\int_{-\pi}^{\pi} e^{-|\mathbf{p}-\gamma(z)|^2/2\sigma^2} |\partial_x \gamma(z)| dz \approx \frac{\sqrt{2\pi}\sigma}{\sqrt{1 - s\kappa_\gamma(z_0)}} e^{-s^2/2\sigma^2},$$

where $s = |\mathbf{p} - \gamma(z_0)|$ is the minimal distance (or separation) between γ and $\mathbf{p}$ and $\kappa_\gamma(z_0)$ is the curvature of γ at the closest point along the curve. In other words, if σ is small relative to the size of the colony, then the nonlocal integral is dominated by those portions of the second curve lying near the point $\gamma(z_0)$ on γ that achieves the minimal separation. In nondimensionalized variables we may therefore solve

$$[1 - C + \kappa_\gamma(z_0)]\sqrt{1 - s\kappa_\gamma(z_0)} = Ce^{-s^2/2\sigma^2}$$

to estimate the separation s at which a front will arrest. For the two competing colonies in Fig. 2 separated by a linear front, we have $\kappa_\gamma(z_0) = 0$, while $\kappa_\gamma(z_0) = -1/r_f$ for r_f the terminal radius (i.e., at arrest) of the circular colony at the center of Fig. 3. Thus curvature terms do not occur for flat fronts, but lead to an increase in colony separation for radial fronts, as Fig. 3 illustrates. These useful calculations, while elementary, would prove significantly more challenging in the context of a large reaction-diffusion system. It is difficult, if not impossible, to perform them for the model from Ref. [26].

We conclude our case study with an illustration of self-inhibition. We accomplish this analytically for radial single colony inoculations and numerically for nonradial inoculations. Given a single radial colony $\gamma(x,t)$ with self-inhibition given by (2), the dynamics (1) lead to the ordinary differential equation (ODE)

$$r' = 1 - r^{-1} - \sqrt{2\pi} C f_\sigma(r,r)(r/\sigma) \tag{3}$$

for the radius $r(t)$ of the colony, where $f_\sigma(r,R) := \exp\{-(r^2 + R^2)/2\sigma^2\} I_0(rR/\sigma^2)$ and $I_0(s)$ denotes the modified Bessel function of the first kind. Similarly, the coupled system of ODEs

$$\begin{pmatrix} r' \\ R' \end{pmatrix} = \begin{pmatrix} -\left(\frac{1}{r} + 1\right) + \sqrt{2\pi} C (r f_\sigma(r,r) + R f_\sigma(r,R))/\sigma \\ 1 - \frac{1}{R} + \sqrt{2\pi} C (r f_\sigma(r,R) + R f_\sigma(R,R))/\sigma \end{pmatrix}$$

describes the evolution of a single annular colony with inner and outer radii $r < R$, respectively. The model (1) therefore

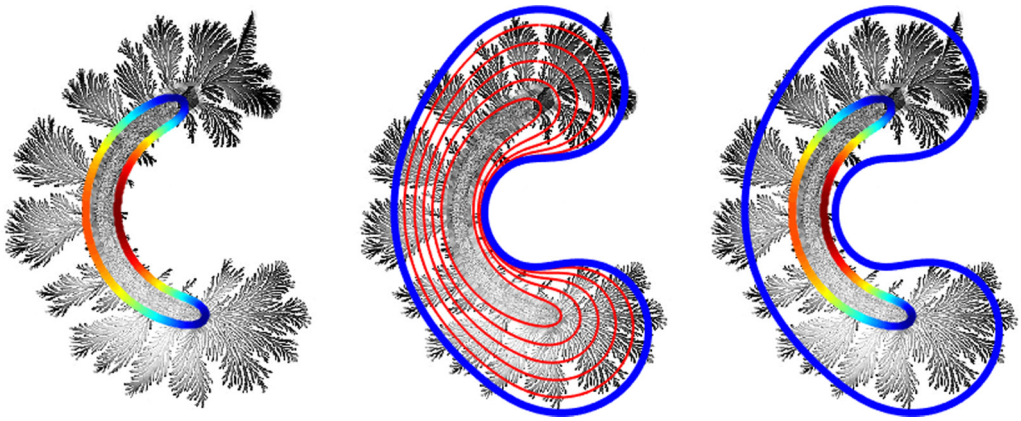

FIG. 4. Dynamics of the model (1) for a single, self-inhibiting colony. The underlying experimental image is from Ref. [25], Fig. 6. At left: An initial inoculation consisting of a half circle of radius 183 connected to a larger half circle of radius 238. Colors indicate the magnitude of the total nonlocal forcing $\mathbf{v}_{\mathrm{NL}}$ at each point; the dark gray regions around the tips of the C are small nonlocal forcing and the dark gray at the C's center are large nonlocal forcing. At center: The evolution of the initial colony under (1), with red (light gray) and blue (dark gray) lines representing time slices from (1) using $(C,\sigma) = (0.464,200)$ and a Gaussian kernel. At right: The initial and final states of the evolution. Smaller values of $|\mathbf{v}_{\mathrm{NL}}|$ do not deter colony growth, while for larger values of $|\mathbf{v}_{\mathrm{NL}}|$ the effect of self-inhibition leads to regions of near zero growth near the center of the colony (a quasiarrested front). (Figure is reproduced with permission.)

illustrates that colony die-out will occur for $r(0)$ sufficiently small, while (3) itself reveals the influence of the self-inhibition strength C and length scale σ on an isolated colony in terms of its die-out radius. The forcing term $f_\sigma(r,R)$ acts with greater strength on the inner radius of an annular colony, which shows that growth of the outer edge can occur while the inner edge remains stagnant, in accordance with experiment (Ref. [25], Fig. 6). Finally, in Fig. 4 we numerically explore the ability of (1) to model the dynamics of self-inhibition for a more complex initial geometry taken from Ref. [25]. When taken together, these results indicate that two simple mechanisms suffice for qualitatively describing the growth of competing bacterial colonies. A curvature mediated constant growth combined with a repulsive force are enough to dictate the overall growth pattern of the colonies. The key parameters therefore are the curvature dependence of a single colony's growth rate, the length scale over which competing colonies can communicate, and the strength of mutual interaction. In particular, the detailed interactions between numerous other compounds are superfluous at the qualitative level.

Conclusions. Nonlocal effects play a key role in many biological systems, and they arise naturally from a plethora of different mechanisms. Our results reveal how nonlocal models can aid our understanding of patterns formed by counterpropagating, interacting fronts that experience arrested motion. While we illustrate this approach using a well-known phenomenon in bacterial colony formation, we emphasize that similar systems are ubiquitous in nature and we expect our approach could be beneficially applied. Examples include multiscale models for tumor growth, wound healing, and angiogenesis [28,29]. Predator-prey systems are also increasingly modeled with nonlocal systems because of the ubiquity of superdiffusion in nature. Desert plants will often inhibit competitor growth in nearby regions to secure more resources such as water [30,31]. Singularly perturbed or nonlocal reaction-diffusion equations have a long history in neuroscience [12–15,32–34]. Moving away from biology, optics has long been a source of singularly perturbed systems where such behavior has been observed (Ref. [35], Figs. 3–7). Indeed, a whole host of physical problems could be explored with our methodology. While reducing a given set of continuum equations to our nonlocal framework is a nontrivial task, directly extracting the tangential, curvature, and nonlocal terms from data is generally more tractable than developing a full set of equations for all possible signaling variables. The pattern forming process for complicated initial geometries can then easily be explored numerically. We are not aware of a similar approach to understanding nonlocal pattern formation; this leaves the door open for many explorations both of the general mathematical behavior of our system and its possible applications for different experimental systems.

Finally, the basic modeling framework (1) has experimental implications in many instances. For example, systems that evolve by mean curvature frequently exhibit self-similar coarsening for different phases or droplets, as is typified in a spinodal decomposition. If the different coarsening domains exhibit a weak interaction as in (1), then we would expect deviations from standard scaling laws predicted by mean-curvature flow alone, and in some cases an unexpected termination of the coarsening process. These deviations can be explicitly measured. A second example concerns the characteristic shape of stable spiral waves that are seen in excitable media such as the heart. The prevailing theory is that this arises from an invariant shape under mean-curvature dynamics, i.e., a purely local and geometric effect. Our approach implies that a nonlocal interaction between arms of the spiral is necessary for the stable spiral shape, and that such coherent behavior then depends crucially on the effective nonlocal interactions in these systems.

This research was supported by National Science Foundation Grant No. DMS-1312344/DMS-1521138.

[1] C. M. Topaz, M. R. D'Orsogna, L. Edelstein-Keshet, and A. J. Bernoff, PLoS Comput. Biol. **8**, e1002642 (2012).
[2] A. L. Bertozzi, J. Rosado, M. B. Short, and L. Wang, J. Stat. Phys. **158**, 647 (2015).
[3] R. Eftimie, J. Math. Biol. **65**, 35 (2012).
[4] C. M. Topaz and A. L. Bertozzi, SIAM J. Appl. Math. **65**, 152 (2004).
[5] A. Mogilner and L. Edelstein-Keshet, J. Math. Biol. **38**, 534 (1999).
[6] C. M. Topaz, A. L. Bertozzi, and M. A. Lewis, Bull. Math. Biol. **68**, 1601 (2006).
[7] S. Motsch and E. Tadmor, J. Stat. Phys. **144**, 923 (2011).
[8] G. M. Viswanathan, V. Afanasyev, S. Buldyrev, E. Murphy, P. Prince, H. E. Stanley *et al.*, Nature (London) **381**, 413 (1996).
[9] D. W. Sims, E. J. Southall, N. E. Humphries, G. C. Hays, C. J. Bradshaw, J. W. Pitchford, A. James, M. Z. Ahmed, A. S. Brierley, M. A. Hindell *et al.*, Nature (London) **451**, 1098 (2008).
[10] N. E. Humphries, N. Queiroz, J. R. Dyer, N. G. Pade, M. K. Musyl, K. M. Schaefer, D. W. Fuller, J. M. Brunnschweiler, T. K. Doyle, J. D. Houghton *et al.*, Nature (London) **465**, 1066 (2010).
[11] S. Chaturapruek, J. Breslau, D. Yazdi, T. Kolokolnikov, and S. McCalla, SIAM J. Appl. Math. **73**, 1703 (2013).
[12] B. Ermentrout, Rep. Prog. Phys. **61**, 353 (1998).
[13] P. C. Bressloff and Z. P. Kilpatrick, Phys. Rev. E **78**, 041916 (2008).
[14] D. J. Pinto and G. B. Ermentrout, SIAM J. Appl. Math. **62**, 206 (2001).
[15] P. C. Bressloff, J. D. Cowan, M. Golubitsky, P. J. Thomas, and M. C. Wiener, Philos. Trans. R. Soc., B **356**, 299 (2001).
[16] J. Carr and R. L. Pego, Commun. Pure Appl. Math. **42**, 523 (1989).
[17] R. L. Pego, Proc. R. Soc. London, Ser. A **422**, 261 (1989).
[18] P. van Heijster, A. Doelman, T. J. Kaper, and K. Promislow, SIAM J. Appl. Dyn. Syst. **9**, 292 (2010).
[19] A. J. Majda and A. L. Bertozzi, *Vorticity and Incompressible Flow*, Vol. 27 (Cambridge University Press, Cambridge, UK, 2002).
[20] H. Sun, D. Uminsky, and A. L. Bertozzi, SIAM J. Appl. Math. **72**, 382 (2012).
[21] K. J. Lee, W. McCormick, Q. Ouyang, and H. L. Swinney, Science **261**, 192 (1993).
[22] D. M. Petrich and R. E. Goldstein, Phys. Rev. Lett. **72**, 1120 (1994).
[23] R. E. Goldstein, D. J. Muraki, and D. M. Petrich, Phys. Rev. E **53**, 3933 (1996).
[24] M. Alfaro, D. Hilhorst, and H. Matano, J. Differ. Equations **245**, 505 (2008).
[25] A. Be'Er, H. Zhang, E.-L. Florin, S. M. Payne, E. Ben-Jacob, and H. L. Swinney, Proc. Natl. Acad. Sci. USA **106**, 428 (2009).
[26] A. Be'er, G. Ariel, O. Kalisman, Y. Helman, A. Sirota-Madi, H. Zhang, E.-L. Florin, S. M. Payne, E. Ben-Jacob, and H. L. Swinney, Proc. Natl. Acad. Sci. USA **107**, 6258 (2010).
[27] Multimedia gallery - colonies of bacteria do battle (image 4)|nsf - national science foundation, http://www.nsf.gov/news/mmg/mmg_disp.jsp?med_id=67192&from=mmg, accessed: 2016-05-09.
[28] K. Harley, P. van Heijster, R. Marangell, G. Pettet, and M. Wechselberger, SIAM J. Appl. Dyn. Syst. **13**, 366 (2014).
[29] K. Harley, P. van Heijster, R. Marangell, G. Pettet, and M. Wechselberger, Nonlinearity **27**, 2975 (2014).
[30] D. L. Phillips and J. A. MacMahon, J. Ecol. **69**, 97 (1981).
[31] B. E. Mahall and R. M. Callaway, Proc. Natl. Acad. Sci. USA **88**, 874 (1991).
[32] G. B. Ermentrout and D. H. Terman, *Mathematical Foundations of Neuroscience*, Vol. 35 (Springer, Berlin, 2010).
[33] J. J. Tyson and J. P. Keener, Physica D: Nonlinear Phenom. **32**, 327 (1988).
[34] J. Nagumo, S. Arimoto, and S. Yoshizawa, Proc. IRE **50**, 2061 (1962).
[35] P. Van Heijster and B. Sandstede, RIMS Kôkyûroku Bessatsu B **31**, 135 (2012).